2013 21st Mediterranean Conference on Control & Automation (MED)
Platanias-Chania, Crete, Greece, June 25-28, 2013

Design of Depth of Anesthesia Controllers in the Presence of Model Uncertainty*

Daniela V. Caiado[1], João M. Lemos[2], Bertinho A. Costa[3], Margarida M. Silva[4] and Teresa F. Mendonça[5]

Abstract— **A major obstacle in the design of controllers to regulate the depth of anesthesia (DoA) consists in the high model uncertainty due to inter-patient variability. Surprisingly, the use of control design methods that explicitly tackle this problem is almost absent from the literature on automatic control of anesthesia. In this work, a DoA controller is designed taking into account model uncertainty to comply with robust stability and robust performance specifications for a patient population undergoing elective general surgery, with hypnosis induced by the drug *propofol*. Due to its Wiener nonlinear structure, the DoA model can be linearized around a given operating point. Therefore, using a database with 18 patient models, a non-parametric description of uncertainty for a linearized model is first performed. By using H_∞ design methods, a continuous linear controller is then designed so as to ensure robust stability and performance within the uncertainty bounds defined. The controller that results from this procedure is approximated by a controller with a lower order that, in turn, is redesigned in discrete time for computer control application. The final result is tested in nonlinear realistic patient models, with acceptable closed-loop results.**

I. INTRODUCTION

To prevent patient awareness during a surgical procedure, hypnosis or depth of anesthesia (DoA) is induced with the administration of hypnotics. The appropriate dosage of these drugs is an important issue for the patient well-being, since an aware state of the patient, as a result of under-dosing, may cause serious long-term psychological consequences, whereas the overdosage may be harmful with respect to postoperative morbidity and mortality. The current anesthetic procedure to induce and maintain the DoA level is mainly based on recommended dosages, according to the patient characteristics, and on the anesthetist experience.

The automatic control of DoA is now a possibility due to the use of the electroencephalogram signal, resulting in measures such as the bispectral index (BIS) [1].

Several control techniques have been studied for DoA using the BIS index as the measured variable, namely, proportional-integral-derivative controllers (PID) [2], model predictive control (MPC) [3], adaptive control [4], [5], neural [6] and fuzzy logic [7] control, in which case the results show the potential to reduce the amount of drug and to maintain hypnosis more accurately than the open-loop control performed with the current clinical practice.

The drug effect on the patient is highly dependent on the patient himself, that leads to high uncertainty levels for the automatic control design. This motivates the use of robust control design techniques in order to design a controller with the appropriate performance to tackle these uncertainties.

Robust control techniques applied to DoA, though scarcely, have been reported in the bibliography, with predictive control [8] and with PID tuning control [9]. Internal model control (IMC) has been explored in [10], indicating better performances with patient uncertainties, compared to the ones obtained with a PID controller. A robust deadbeat controller is designed in [11] that shows an improved performance in over/undershooting and settling time when compared with the performances of two PID based controllers.

The problem of DoA control design in the presence of model uncertainties and unmodeled dynamics is addressed in this paper. The controller is designed based on H_∞ theory and is such as to provide an adequate drug administration, with a good reference tracking and an output disturbance rejection, while stabilizing the class of possible patient models within the uncertainty bounds considered.

The paper is organized as follows. After this introduction, the mathematical model is described in section II and the control design method is presented in section III, where robust performance and robust stability are considered. Conclusions are drawn is section IV.

II. PHARMACOKINETIC / PHARMACODYNAMIC MODEL FOR *PROPOFOL*

Models for *propofol* have been the subject of several publications [12], [13], [14]. This section describes the particular models used in a state-space form that is suitable for the purpose of this work.

The effect of the hypnotic drug on the patient can be modeled by the interaction of three compartments, a central

*This work was performed in the framework of the project GALENO, funded by FCT (Fundação para a Ciência e a Tecnologia, Portugal) under contract PTDC/SAU-BEB/103667/2008, and PEst - OE/EEI/LA0021/2011. This work was supported in part by the European Research Council via the Advanced Grant 247035; by FEDER funds through COMPETE–Programa Operacional Factores de Competitividade, and by Portuguese funds through the Center for Research & Development in Mathematics and Applications and FCT, within project PEst-C/MAT/UI4106/2011 with COMPETE number FCOMP-01-0124-FEDER-022690.

[1]D. V. Caiado is with INESC-ID, Lisboa, Portugal danielavcaiado at gmail.com

[2]J. M. Lemos is with INESC-ID and IST/UTL, Rua Alves Redol 9, 1000-029 Lisboa, Portugal jlml at inesc-id.pt

[3]B. A. Costa is with INESC-ID and IST/UTL, Lisboa, Portugal bac at inesc-id.pt

[4]M. M. Silva is with FCUP, Porto, Portugal; Center for Research & Developments in Mathematics and Applications, Universidade de Aveiro, Portugal, and with the Division of Systems and Control, Department of Information Technology, Uppsala University, Sweden margarida.silva at fc.up.pt

[5]T. F. Mendonça is with FCUP, Porto, Portugal and with the Center for Research & Developments in Mathematics and Applications, Aveiro, Portugal tmendo at fc.up.pt

compartment where the drug is perfused, and two peripheral compartments (Fig. 1).

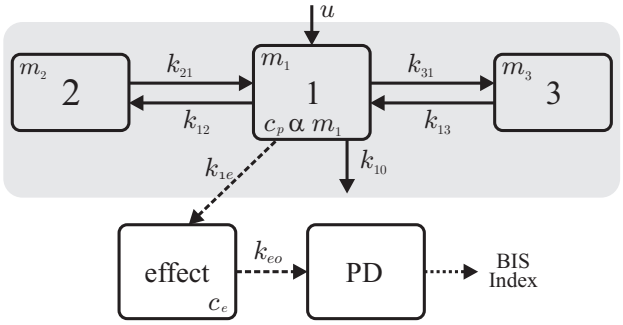

Fig. 1. Schematic representation of the compartmental model for the dynamic response of hypnosis. The shadowed region is the PK part of the model.

One of the peripheral compartments represents the fast distribution of the drug from the central compartment to the muscles and organs, and the other represents the bones and fat tissue to where the drug distribution is slow. These interactions form the pharmacokinetic model (PK) of the drug, as it relates the drug dose u (ml/h) administered to the patient with the plasma concentration of the drug c_p (μg/ml). The mathematical model that describes the drug-patient pharmacokinetics is written in state-space form as

$$\begin{cases} \dot{m_1}(t) = -k_{10}m_1(t) - k_{12}m_1(t) - k_{13}m_1(t) \\ \qquad +k_{21}m_2(t) + k_{31}m_3(t) + \frac{1000}{60}u(t) \\ \dot{m_2}(t) = k_{12}m_1(t) - k_{21}m_2(t) \\ \dot{m_3}(t) = k_{13}m_1(t) - k_{31}m_3(t) \\ c_p(t) = \frac{1}{1000\times V_1}m_1(t) \end{cases}, \quad (1)$$

where m_i (μg), with $i = 1, 2, 3$, is the mass in the compartment i, k_{ij} (min^{-1}) is the equilibrium constant from the i-th to the j-th compartment and V_1 (l) is the volume of the central compartment.

The relationship between the plasma concentration of the drug and its actual effect is referred to as the pharmacodynamic model (PD). The PD model encompasses the relation between the plasma concentration and the concentration in the effect compartment, and the relation between this last variable and the DoA level. The drug concentration in the effect compartment c_e (μg/ml) is described by

$$\dot{c_e} = -k_{eo}c_e + k_{1e}c_p, \quad (2)$$

where k_{1e} (min^{-1}) is the equilibrium constant between the central and the effect compartments that is considered to be equal to k_{eo} which represents the removal of the drug from the body. The model constants are computed with the Schnider model [15] for the database considered in this work. The Schnider model depends on weight (w), height (h), gender (within the computation of the lean body mass - LBM) and age, with parameters given by

$$V_1 = 4.27 \quad \text{(l)} \quad (3)$$

$$V_2 = 18.9 - 0.391\ (age - 53) \quad \text{(l)} \quad (4)$$

$$V_3 = 238 \quad \text{(l)} \quad (5)$$

$$L_1 = 1.89 - 0.0456\ (w - 77) - 0.0681\ (LBM - 59) + 0.0264\ (h - 177) \quad \text{(l/min)} \quad (6)$$

$$L_2 = 1.29 - 0.024\ (age - 53) \quad \text{(l/min)} \quad (7)$$

$$L_3 = 0.836 \quad \text{(l/min)} \quad (8)$$

$$k_{eo} = 0.456 \quad (\text{min}^{-1}), \quad (9)$$

where

$$LBM = 1.1 \times w - 128\left(\frac{w}{h}\right)^2 \quad \text{(Male)} \quad (10)$$

$$LBM = 1.07 \times w - 148\left(\frac{w}{h}\right)^2 \quad \text{(Female)}, \quad (11)$$

and

$$L_1 = V_1\ k_{10} \quad (12)$$

$$L_2 = V_2\ k_{21} \quad (13)$$

$$L_3 = V_3\ k_{31} \quad (14)$$

$$V_2 = V_1\frac{k_{12}}{k_{21}} \quad (15)$$

$$V_3 = V_1\frac{k_{13}}{k_{31}}, \quad (16)$$

where L_i, with $i = 1, 2, 3$, is the clearance that is defined as the volume of plasma from which the drug is completely removed per unit time. Variables V_2 and V_3 are the volumes of the fast and slow compartments, respectively.

The drug effect observed on the patient may be expressed as a nonlinear function of the effect compartment concentration, such as

$$BIS = E_0 + (E_{max} - E_0)\frac{c_e^\gamma}{c_e^\gamma + C_{50}^\gamma}, \quad (17)$$

where E_0 is the baseline effect at zero concentrations, E_{max} is the peak drug effect, C_{50} is the concentration related with 50 % of the drug effect and γ is the steepness of the concentration-response relation.

Bouillon *et al.* outlined in [16] that there is a synergetic effect between the analgesic drug *remifentanil* and the hypnotic drug *propofol* that is revealed in the electroencephalographic measure BIS. This synergic relationship can be expressed in the overall effect as

$$BIS = \frac{97.7}{1 + ((1+\beta)\,U^{prop} + U^{remi})^\gamma}, \quad (18)$$

where β is a patient dependent parameter and U^{prop} and U^{remi} are the normalized effect concentrations defined as

$$U^{prop} = \frac{c_e^{prop}}{C_{50}^{prop}}, \qquad U^{remi} = \frac{c_e^{remi}}{C_{50}^{remi}}, \quad (19)$$

where the super-index *prop* refers to the variables associated with *propofol* and the hypnotic model, whereas the super-index *remi* refers to the variables associated with *remifentanil* and the analgesic model. In this work, the *remifentanil* dose appears in the model as a disturbance. Although one could take advantage of knowing its value, this feedforward term is not considered in this work

A. Linear model for DoA

The linear part of the model (1,2) that relates the drug dose u with the effect compartment concentration, is described by the state-space model

$$\begin{cases} \dot{x}(t) = \Phi\ x(t) + \Gamma\ u(t) \\ c_e(t) = \mathbb{I}\ x(t) \end{cases}, \tag{20}$$

where Φ is a patient dependent matrix defined as

$$\Phi = \begin{bmatrix} -(k_{10}+k_{12}+k_{13}) & k_{21} & k_{31} & 0 \\ k_{12} & -k_{21} & 0 & 0 \\ k_{13} & 0 & -k_{31} & 0 \\ \frac{k_{eo}}{1000\times V_1} & 0 & 0 & -k_{eo} \end{bmatrix}, \tag{21}$$

x is the state defined as

$$x = \begin{bmatrix} m_1 \\ m_2 \\ m_3 \\ c_e \end{bmatrix}, \quad \Gamma = \begin{bmatrix} \frac{1000}{60} \\ 0 \\ 0 \\ 0 \end{bmatrix}, \quad \mathbb{I} = \begin{bmatrix} 0 & 0 & 0 & 1 \end{bmatrix}, \tag{22}$$

and t is the continuous time measured in minutes.

In the Laplace transform domain, the state-space system (20) is described by

$$c_e(s) = F(s)u(s), \tag{23}$$

where $F(s)$ is the transfer function of the linear part of the model and s is the Laplace variable.

The nonlinear relationship between the effect compartment concentration and the DoA level only affects the static gain of the linearized model, yielding two sources of uncertainties: change of the derivative with respect to the equilibrium point and parameters variability. After a linear approximation by the Jacobian linearization of the nonlinear description of the dependence of the observed effect (18) on the effect compartment concentration, the patient response is described by

$$BIS(s) = F(s)\ \eta\ u(s) = G(s)\ u(s), \tag{24}$$

where η is given by the derivative of BIS, in (18), with respect to c_e^{prop}, and $G(s)$ is the transfer function that relates the patient response, measured by the BIS index, with the drug dose. The variable η represents the static gain of the nonlinear term of the model, and relates the increment of the drug effect-site concentration with its effect given by the increment of the BIS index, with respect to its equilibrium value.

III. CONTROL DESIGN

In a surgical procedure, the BIS index should be around 50 and kept over the threshold of 30 all the time, to prevent postoperative morbidity.

An automatic feedback control system, as the one shown in Fig. 2, can be implemented, where the controller (K) is designed to compare the value of the BIS index (y) with the desired level (r), and to compute the amount of drug (u) required to deliver to the patient. The drug is administered to the patient through a syringe that is commanded by the computer, that samples the BIS index value every 5 seconds. In this control system (Fig. 2), the noise sensor (n) and load disturbances (d) are considered, and the controller is designed to have integral action in order to overcome possible steady-state errors.

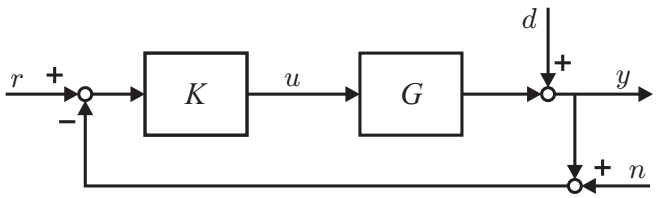

Fig. 2. Schematic representation of the control system

The closed-loop patient response is

$$y = \frac{1}{1+KG}\ d + \frac{KG}{1+KG}\ r - \frac{KG}{1+KG}\ n. \tag{25}$$

The transfer function from d to y is the sensitivity function, $S(s)$, and the transfer function from r to y is the complementary sensitivity function, $T(s)$. The transfer function $n \to y$ is $-T(s)$.

In the work described here, the H_∞ control design technique is used to design a suitable controller for this problem [17]. The H_∞ method approaches the control problem as an optimization problem in the frequency domain, in order to yield the desired time domain response. The main goal is to obtain a controller that is able to yield robust performance as well as robust stability, in the presence of model uncertainty.

The model uncertainty can be characterized as a multiplicative uncertainty, with respect to the nominal model G_N, from which a true model G can be computed as

$$G(j\omega) = G_N(j\omega)(1 + \Delta(j\omega)), \tag{26}$$

where Δ is the multiplicative uncertain dynamics at frequency ω. In this work, a database of 18 models are set to be used in the design of the robust controller. The patients in this database have health features corresponding to levels I to IV according to the American Society of Anesthesiology, being subject to elective surgery. The data was originally collected to other studies that satisfy ethics requirements. The dynamic behavior of these models is highly diverse, as shown by the frequency response of Fig. 3

A. Robust Performance

For robust performance, the described system in (25) is designed to reject load disturbances and sensor noise, in the presence of model uncertainty. The load disturbance rejection objective is defined as a weighted sensitivity minimization problem and the sensor noise rejection objective is defined as a weighted complementary sensitivity minimization problem. This is accomplished by introducing weighting functions in the closed-loop response that behave as boundaries for the models sensitivity functions (S) and complementary sensitivity functions (T).

The two performance goals are closely related through the specification of the controlled system bandwidth (by the

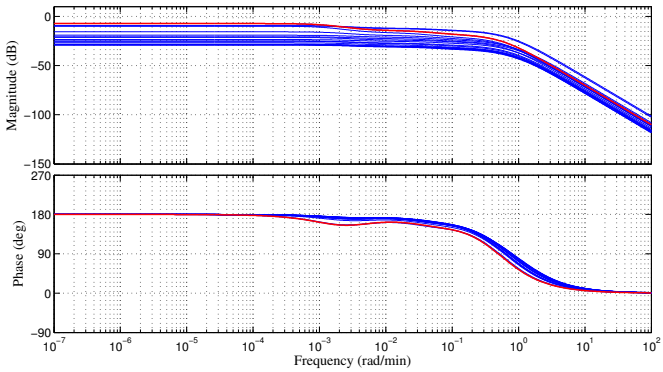

Fig. 3. Frequency response of all the $G(s)$ models in the patient bank. The nominal model is represented in red.

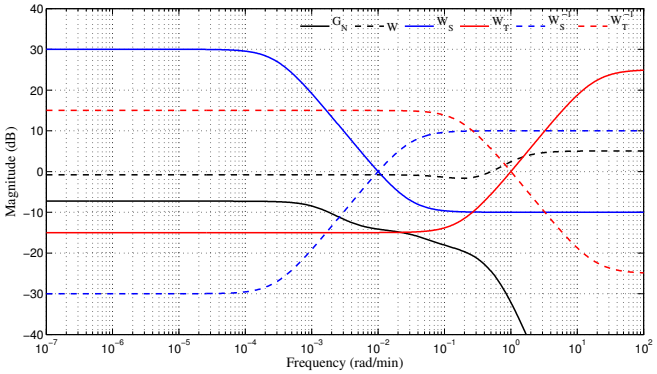

Fig. 5. Magnitude of the weighting functions W_S and W_T, and of the respective inverse functions W_S^{-1} and W_T^{-1}. The nominal model G_N and the cover W (upper bound function) of all uncertainties of model G_i are also shown.

sensitivity function), and reference tracking and robust stability specifications (related to the complementary sensitivity function). The weighted system is,

$$y = \frac{1}{1+KG}\, W_S\; d + \frac{KG}{1+KG}\; r - \frac{KG}{1+KG}\; W_T\; n, \quad (27)$$

as depicted in Fig. 4, where W_S and W_T affect the sensitivity and the complementary sensitivity functions, respectively Thus, for the load disturbance rejection performance, the gain

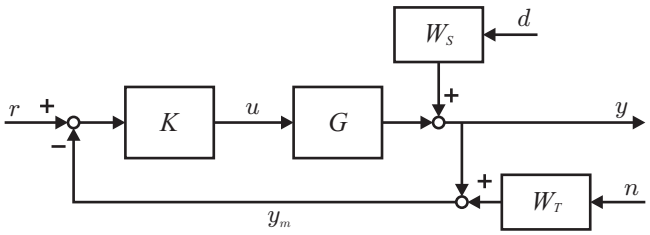

Fig. 4. Schematic representation of the control action with the weighting functions.

of the weighted sensitivity function must be kept below 1, implying that

$$|S.W_S| < 1 \qquad \Leftrightarrow \qquad |S| < \frac{1}{|W_S|}. \quad (28)$$

This weighted sensitivity function enforces the desired bandwidth, while the weighted complementary sensitivity function enforces the adequate roll-off outside the bandwidth in which the disturbances are rejected.

The noise rejection problem is approached in the same way, as the gain of the weighted complementary sensitivity function must be kept below 1, so that

$$|T.W_T| < 1 \qquad \Leftrightarrow \qquad |T| < \frac{1}{|W_T|}. \quad (29)$$

Conditions (28) and (29) must be satisfied for each S_i and T_i, with $i = 1, ..., 18$ of all the G_i models. In this case, the weighting functions W_S and W_T are selected to have the frequency response shown in Fig. 5.

The weight W_T^{-1} is a low-pass function whose shape is selected such as to ensure reference tracking up to the desired bandwidth (that implies that W_T^{-1} is small) and noise rejection in the higher frequency band, as well as robustness with respect to high frequency model uncertainty (that implies that W_T^{-1} is high in this band) [17]. A dual behavior follows to W_S^{-1}.

B. Robust Stability

The robust stability objective consists in the design of a stabilizing controller for all the plant models in the given class of the 18 models. Thus, for robust stability analysis, the Nyquist stability criterion is called upon. Based on this criterion, the controller K designed to stabilize the nominal model G_N, also stabilizes G if

$$|KG_N(j\omega) - KG(j\omega)| < |1 + KG_N(j\omega)|\,. \quad (30)$$

This is called the robust stability condition.

With (26), condition (30) can be written in the form

$$|\Delta(j\omega)| < \frac{|1 + KG_N(j\omega)|}{|KG_N(j\omega)|}. \quad (31)$$

Let $l(\omega)$ be an upper bound function of the multiplicative uncertainty, meaning that

$$|\Delta(j\omega)| = \frac{|KG_N(j\omega) - KG(j\omega)|}{|KG_N(j\omega)|} < l(\omega). \quad (32)$$

Therefore, if $l(\omega)$ is such that

$$l(\omega) < \frac{|1 + KG_N(j\omega)|}{|KG_N(j\omega)|}, \quad (33)$$

condition (30) is satisfied, and all the models that verify (32) will be stabilized by the controller K.

Condition (33) may be written in the form

$$\frac{1}{l(\omega)} > \frac{|KG_N(j\omega)|}{|1 + KG_N(j\omega)|} = |T_N(j\omega)|\,, \quad (34)$$

where T_N is the complementary sensitivity function obtained with the nominal model and corresponds to the closed-loop transfer function obtained when the controller is coupled with the nominal model. Thus, if an upper bound function $l(\omega)$ for the multiplicative uncertainties exists such that $l^{-1}(\omega)$

is also an upper bound for the complementary sensitivity function, the controller designed for the nominal model has robust stability, meaning that all the systems G_i that satisfy (32) are stabilized by the nominal controller.

C. Controller Synthesis and Analysis

With all the performance and robust stability issues taken into account, the controller synthesis is performed using the DK–algorithm for μ–synthesis, explained in [17], in the implementation provided by the function `dksyn` of MATLAB®, that is described by *Robust Control Toolbox* ™ User's Guide [18]. The controller description is a state-space model expressed as

$$\begin{cases} \dot{x_c}(t) = A\ x_c(t) + B\ e(t) \\ u(t) = C\ x_c(t) \end{cases}, \tag{35}$$

where A, B and C are the matrices that result from the design algorithm, e is the tracking error, $e = r - y_m$, and x_c is the controller state.

The resulting controller stabilizes all models, if the loop gain, verifies

$$|KG(j\omega)| < 1 \qquad \text{at} \qquad \angle KG(j\omega) = -180^\circ, \tag{36}$$

where $|KG(j\omega)|$ is the gain and $\angle KG(j\omega)$ is the phase, is fulfilled for all G_i, with $i = 1, ..., 18$.

The controller yields the desired performance, since the weighting functions W_S and W_T are the upper bounds of all models sensitivity functions and complementary sensitivity functions, respectively, as shown in Fig. 6.

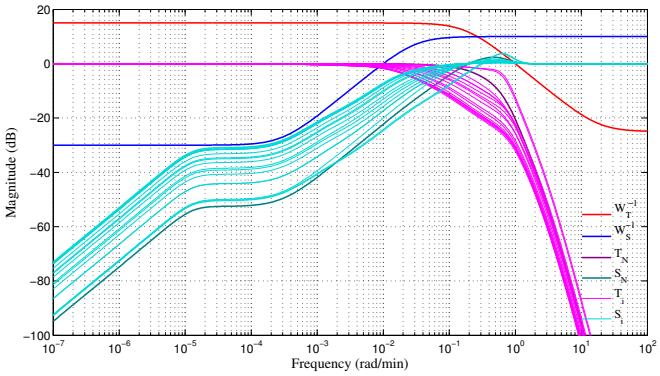

Fig. 6. Gain of the sensitivity functions S and the complementary sensitivity functions T, with the upper bounds W_S^{-1} and W_T^{-1}. This plot is used to check the robust performance conditions.

The robust stability condition, that relies on the existence of an upper bound function $l(\omega)$ that yields conditions (32) and (34), is fulfilled as shown in Fig. 7 and 8, as the function $l(\omega)$ and its inverse are, respectively, the upper bound of all uncertainties and of the nominal complementary sensitivity function.

The resulting controller has 20 states and is approximated by a 8$^{\text{th}}$– order controller, preserving all system characteristics in the frequency range of interest, as shown by the frequency response of Fig. 9.

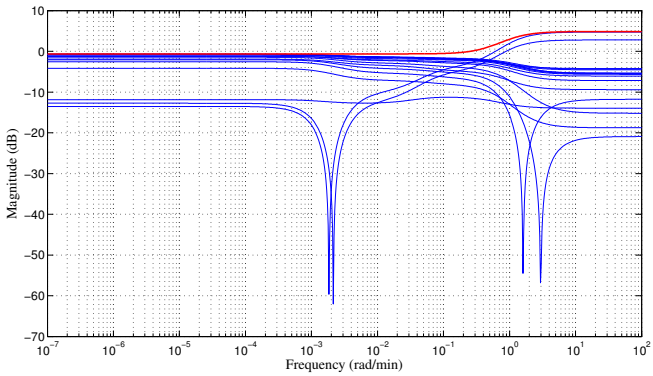

Fig. 7. Magnitude of the multiplicative uncertainty Δ of the open-loop controlled systems. The function $l(\omega)$ is represented in red.

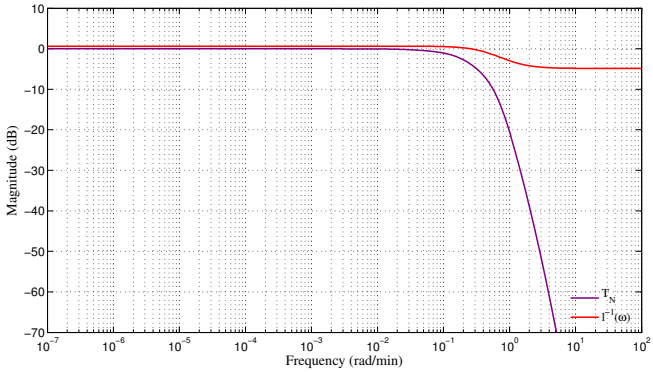

Fig. 8. Gain of the inverse upper bound function for multiplicative uncertainty $l^{-1}(\omega)$ and the nominal complementary sensitivity function T_N. This plot is used to verify the robust stability condition.

The controller is redesigned in discrete time, with a sampling time of 5 seconds, and the resulting controller ensures robust performance and robust stability.

The time response of Fig. 10 shows the controller action and the system response for all models, where it is possible to conclude that the controller is able to provide acceptable performances in reference tracking and noise rejection, as well as stabilizing all the models.

IV. CONCLUSIONS

An approach to the design of robust controllers for DoA based on H_∞ design and μ–synthesis has been proposed and illustrated using a bank of patient data. The approach consists in characterizing a multiplicative uncertainty model description for a set of patients, enlarging this model with an integrator to ensure zero steady-state tracking error, controller design using the DK–algorithm, controller order reduction, and controller redesign in discrete time to obtain a controller suitable for computer application.

The controller that is designed aiming at robust performance and stability is able to track the reference for all the models. The performance conditions are satisfied for all the models, since the sensitivity functions and complementary sensitivity functions fall below the bounds W_S^{-1} and W_T^{-1}, respectively. This controller has robust stability for the 18

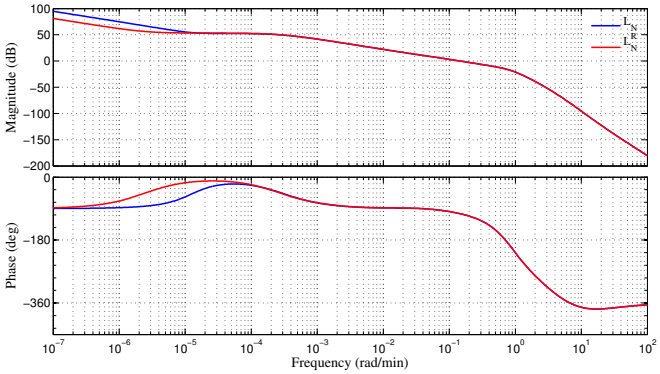

Fig. 9. Gain of the open-loop controlled nominal model with the full order controller and with the reduced-order controller (L_N^R).

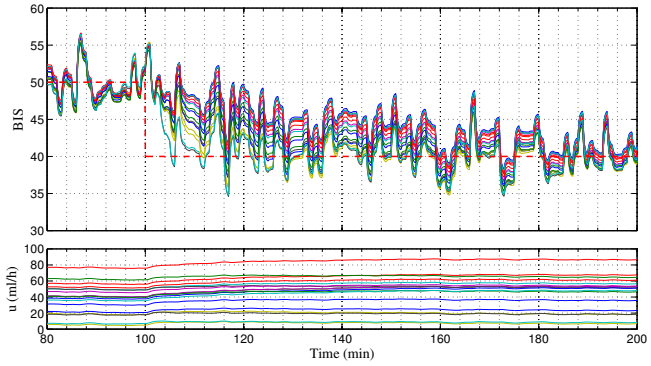

Fig. 10. Simulated time response of the controlled systems and the control action (u) for all models. The reference is represented by the red dashed line. An initial dose (not shown) is infused for fast induction of DoA, followed by an initial constant infusion computed to maintain BIS at 50 %. The controller is switched on. A step on the reference value from 50 % to 40 % is performed at 100 min. The drug concentration is 20 mg/ml.

models of the database, yielding appropriate time responses with simulated noise as to mimic the real sensor noise.

The order reduction and the *a posteriori* discretization allows computer control application.

REFERENCES

[1] L. A. Kearse Jr, C. Rosow, A. Zaslavsky, P. Connors, M. Dershwitz, and W. Denman, "Bispectral analysis of the electroencephalogram predicts conscious processing of information during propofol sedation and hypnosis." *Anesthesiology*, vol. 88, no. 1, pp. 25–34, Jan. 1998.

[2] A. Absalom, N. Sutcliffe, and G. N. Kenny, "Closed-loop control of anesthesia using bispectral index: performance assessment in patients undergoing major orthopedic surgery under combined general and regional anesthesia," *Anesthesiology*, vol. 96, no. 1, pp. 67–73, Jan. 2002.

[3] Y. Sawaguchi, E. Furutani, G. Shirakami, M. Araki, and K. Fukuda, "A model-predictive hypnosis control system under total intravenous anesthesia," *IEEE Transactions on Biomedical Engineering*, vol. 55, no. 3, pp. 874 –887, Mar. 2008.

[4] C. S. Nunes, T. Mendonça, J. M. Lemos, and P. Amorim, "Feedforward adaptive control of the bispectral index of the EEG using the intravenous anaesthetic drug propofol," *International Journal of Adaptive Control and Signal Processing*, vol. 23, no. 5, pp. 485–503, May 2009.

[5] M. M. Silva, T. Wigren, and T. Mendonça, "Exactly linearizing adaptive control of propofol and remifentanil using a reduced wiener model for the depth of anesthesia," in *Decision and Control (CDC), 2012 IEEE 51st Annual Conference on*, Dec. 2012, pp. 368 –373.

[6] O. Ortolani, A. Conti, A. Di Filippo, C. Adembri, E. Moraldi, A. Evangelisti, M. Maggini, and S. J. Roberts, "EEG signal processing in anaesthesia. use of a neural network technique for monitoring depth of anaesthesia," *British Journal of Anaesthesia*, vol. 88, no. 5, pp. 644–648, May 2002.

[7] J. S. Shieh, D. A. Linkens, and A. J. Asbury, "A hierarchical system of on-line advisory for monitoring and controlling the depth of anaesthesia using self-organizing fuzzy logic," *Engineering Applications of Artificial Intelligence*, vol. 18, no. 3, pp. 307–316, Apr. 2005.

[8] C. M. Ionescu, R. De Keyser, B. C. Torrico, T. De Smet, M. M. Struys, and J. E. Normey-Rico, "Robust predictive control strategy applied for propofol dosing using BIS as a controlled variable during anesthesia," *IEEE Transactions on Biomedical Engineering*, vol. 55, no. 9, pp. 2161–2170, Sep. 2008.

[9] G. A. Dumont, A. Martinez, and J. M. Ansermino, "Robust control of depth of anesthesia," *International Journal of Adaptive Control and Signal Processing*, vol. 23, no. 5, pp. 435–454, May 2009.

[10] S. Anna and P. Wen, "Depth of anesthesia control using internal model control techniques," in *2010 IEEE/ICME International Conference on Complex Medical Engineering*, Jul. 2010, pp. 294–300.

[11] S. Abdulla and P. Wen, "Depth of anaesthesia control investigation using robust deadbeat control technique," in *2012 ICME International Conference on Complex Medical Engineering*, Jul. 2012, pp. 107–111.

[12] B. Marsh, M. White, N. Morton, and G. N. C. Kenny, "Pharmacokinetic model driven infusion of propofol in children," *British Journal of Anaesthesia*, vol. 67, no. 1, pp. 41–48, Jul. 1991.

[13] T. W. Schnider, C. F. Minto, S. L. Shafer, P. L. Gambus, C. Andresen, D. B. Goodale, and E. J. Youngs, "The influence of age on propofol pharmacodynamics." *Anesthesiology*, vol. 90, no. 6, pp. 1502–1516, Jun. 1999.

[14] J. B. Dyck and S. L. Shafter, "Effects of age on propofol pharmacokinetics." in *Seminars in Anesthesia*, vol. 11. Implemented in the computer program Stanpump, May 1992, pp. 2–4.

[15] T. W. Schnider, C. F. Minto, P. L. Gambus, C. Andresen, D. B. Goodale, S. L. Shafer, and E. J. Youngs, "The influence of method of administration and covariates on the pharmacokinetics and pharmacodynamics of propofol in adult volunteers," *Anesthesiology*, vol. 88, no. 5, pp. 1170–82, May 1998.

[16] T. W. Bouillon, J. Bruhn, L. Radulescu, C. Andresen, T. J. Shafer, C. C., and S. L. S., "Pharmacodynamic interaction between propofol and remifentanil regarding hypnosis, tolerance of laryngoscopy, bispectral index, and electroencephalographic approximate entropy," *Anesthesiology*, vol. 100, no. 6, pp. 1353–72, Jun. 2004.

[17] S. Skogestad and I. Postlethwaite, *Multivariable Feedback Control Analysis and Design*. John Wiley & Sons, 2005.

[18] G. Balas, A. Chiang, R. Packard, and M. Safanov, *Robust Control Toolbox™ User' Guide*, The MathWorks, Inc., 2012.